A finite-difference method for orthorhombic reverse time migration

Sang Yong Suh, TGS*

SUMMARY

This paper presents a simple finite-difference method of an acoustic-tilted orthorhombic wave equation for reverse time migration. In this approach, I assume locally constant rotation angles and expanded the wave equation in terms of both mixed and nonmixed second derivatives. The assumption of a zero vertical shear wave velocity introduces instability if conventional finite-difference method is used. Because the instability is due to the presence of the quasi S-waves, a conditional damping term is added to reduce the effects of this instability. This method not only produces a stable solution but also reduces unwanted S-wave noise generated by the source injection and/or by the layer interface. To reduce the source generated noise further, I apply an orthorhombic-elliptic anisotropy condition. Numerical examples show that the proposed method is effective. The method is applied on a Gulf of Mexico field data orthorhombic RTM resulting in a better image than with TTI RTM.

INTRODUCTION

Tsvankin (1997) transformed the nine independent elastic constants for orthorhombic-anisotropic media into the same number of independent Thomsen-style (Thomsen, 1986) anisotropic parameters. Under the acoustic assumption, the number of independent parameters is reduced to six. This reduction allows much simpler seismic data processing and interpretation than with the original elastic constants.

Zhang and Zhang (2011) derived a second-order wave equation for reverse time migration in arbitrary heterogeneous 3D acoustic-orthorhombic media (ORT) with tilted-symmetry axis. To stabilize the numerical method, they used self-adjoint differential operators in rotated coordinates. The self-adjoint operators contain tilted first-order derivatives which are computed using a centered finite-difference scheme. However, the solution could suffer from high-frequency ringing artifacts unless an extremely high-order finite-difference scheme is used.

I present a simple finite-difference implementation of an acoustic-tilted orthorhombic wave equation. However, the method is unstable due to the triplicated quasi S-waves. Understanding that the instability is due to the S-waves, I compute a stable solution by separating P- and S-waves, and selectively attenuate the S-waves so that its amplitude remains small. This method not only gives a stable solution but also reduces unwanted S-wave noise. To further remove the S-wave noise, I derive an orthorhombic elliptic anisotropy condition. I compare the proposed method with several existing methods. A field-data example comparing TTI RTM and orthorhombic RTM is shown.

METHOD

Zhang and Zhang (2011) introduced an orthorhombic wave equation given by

$$\frac{1}{V_p^2}\frac{\partial^2 \boldsymbol{\sigma}}{\partial t^2} = \mathbf{N}\mathbf{D}^T\mathbf{D}\boldsymbol{\sigma} \tag{1}$$

where $\boldsymbol{\sigma} = (\sigma_1, \sigma_2, \sigma_3)^T$ is the principal stress vector, V_p is the P-wave velocity in the vertical axis, $\mathbf{N}$ is the orthorhombic-anisotropic maxtrix defined by

$$\mathbf{N} = \begin{pmatrix} 1+2\varepsilon_2 & (1+2\varepsilon_2)\sqrt{1+2\delta_3} & \sqrt{1+2\delta_2} \\ (1+2\varepsilon_2)\sqrt{1+2\delta_3} & 1+2\varepsilon_1 & \sqrt{1+2\delta_1} \\ \sqrt{1+2\delta_2} & \sqrt{1+2\delta_1} & 1 \end{pmatrix} \tag{2}$$

and $\mathbf{D}$ is the tilted first-order derivative,

$$\mathbf{D} = \begin{pmatrix} R_1^T\nabla & 0 & 0 \\ 0 & R_2^T\nabla & 0 \\ 0 & 0 & R_3^T\nabla \end{pmatrix} \tag{3}$$

with R_i being the column vectors of the orthorhombic rotation matrix, $\mathbf{R}$

$$\mathbf{R} = \begin{pmatrix} \cos\phi & -\sin\phi & 0 \\ \sin\phi & \cos\phi & 0 \\ 0 & 0 & 1 \end{pmatrix} \begin{pmatrix} \cos\theta & 0 & \sin\theta \\ 0 & 1 & 0 \\ -\sin\theta & 0 & \cos\theta \end{pmatrix} \times \begin{pmatrix} \cos\beta & -\sin\beta & 0 \\ \sin\beta & \cos\beta & 0 \\ 0 & 0 & 1 \end{pmatrix}, \tag{4}$$

where θ is the tilt angle, ϕ is the azimuthal angle, and β is the angle between the x-axis and the crack normal.

To simplify the computation, I assume locally constant angles and ignore their derivatives. Expanding the differential operator $\mathbf{D}^T\mathbf{D}$ in equation (1) gives

$$\mathbf{D}^T\mathbf{D} = \begin{pmatrix} d_1 & 0 & 0 \\ 0 & d_2 & 0 \\ 0 & 0 & d_3 \end{pmatrix} \tag{5}$$

where

$$\begin{aligned} d_1 &= r_{11}^2\partial_{xx} + r_{21}^2\partial_{yy} + r_{31}^2\partial_{zz} + 2r_{11}r_{21}\partial_{xy} + 2r_{11}r_{31}\partial_{xz} + 2r_{21}r_{31}\partial_{yz} \\ d_2 &= r_{12}^2\partial_{xx} + r_{22}^2\partial_{yy} + r_{32}^2\partial_{zz} + 2r_{12}r_{22}\partial_{xy} + 2r_{12}r_{32}\partial_{xz} + 2r_{22}r_{32}\partial_{yz} \\ d_3 &= r_{13}^2\partial_{xx} + r_{23}^2\partial_{yy} + r_{33}^2\partial_{zz} + 2r_{13}r_{23}\partial_{xy} + 2r_{13}r_{33}\partial_{xz} + 2r_{23}r_{33}\partial_{yz}. \end{aligned} \tag{6}$$

with r_{ij} being the elements of the rotation matrix $\mathbf{R}$.

Equation (6) contains mixed and nonmixed second derivatives. To evaluate the nonmixed derivative terms, I use 16th order optimized second-derivative finite-difference scheme. The coefficients are derived following Holberg (1987) optimization

DOI http://dx.doi.org/10.1190/segam2014-1290.1

technique. By the way, the mixed terms are less important than the nonmixed terms (Duveneck and Bakker, 2011). Therefore, I use an 8th order centered finite-difference scheme. The finite-difference coefficients were derived following Kindelan et al. (1990)

As in the TTI wave modeling, the above method is unstable. The instability is due to the quasi S-wave. The quasi S-wave is just an auxiliary wave due to the anellipticity. Consequently, its amplitude should be much smaller than that of P-wave unless the anellipticity is abnormally high. To limit the S-wave amplitude, I introduce a conditional damping to equation (1) as follow:

$$\frac{1}{V_p^2}\frac{\partial^2}{\partial t^2}\begin{pmatrix}\sigma_1\\ \sigma_2\\ \sigma_3\end{pmatrix} + \frac{a}{V_p}\frac{\partial}{\partial t}\begin{pmatrix}q_x\\ q_y\\ 0\end{pmatrix} = \mathbf{N}\mathbf{D}^T\mathbf{D}\begin{pmatrix}\sigma_1\\ \sigma_2\\ \sigma_3\end{pmatrix}, \qquad (7)$$

where $q_x = \sigma_1 - \sigma_3$, $q_y = \sigma_2 - \sigma_3$. Here a is a conditional attenuation defined by

$$a = \begin{cases} \alpha & \text{if}\sqrt{q_x^2+q_y^2}/|\sigma_3| > \tau \\ 0 & \text{if}\sqrt{q_x^2+q_y^2}/|\sigma_3| \le \tau \end{cases}$$

where α is the damping constant and τ is the threshold which can be determined from the maximum anellipticity of the earth model.

Equation (7) gives stable solution by limiting the S-wave amplitude. However, reduction of S-wave is time dependent and is effective for later times only. Consequently, the source-generated S-wave noise at early times is not removed effectively. To remove source-generated S-wave noise, I use conventional wisdom, i.e., enforce the elliptic anisotropy around the source point.

I now derive an elliptic anisotropy condition for orthorhombic wave equation. Let us introduce three variables p, q and r which are related to the three principal stress components as follows:

$$\begin{aligned}\sigma_1 &= p + n_{31}r\\ \sigma_2 &= q + n_{32}r\\ \sigma_3 &= r.\end{aligned} \qquad (8)$$

Substituting the above equation into equation (1) and rewriting with respect to the second time derivatives of p, q, r gives:

$$\frac{1}{V_p^2}\frac{\partial^2}{\partial t^2}\begin{pmatrix}p\\ q\\ r\end{pmatrix} = \mathbf{G}\mathbf{D}^T\mathbf{D}\begin{pmatrix}p+n_{31}r\\ q+n_{32}r\\ r\end{pmatrix}, \qquad (9)$$

where the matrix $\mathbf{G}$ is given by

$$\mathbf{G} = \begin{pmatrix} n_{11}-n_{31}^2 & n_{12}-n_{31}n_{32} & 0\\ n_{21}-n_{31}n_{32} & n_{22}-n_{32}^2 & 0\\ n_{31} & n_{32} & 1\end{pmatrix}. \qquad (10)$$

If we define,

$$\begin{aligned}\varepsilon_1 &= \delta_1\\ \varepsilon_2 &= \delta_2\\ \delta_3 &= (\delta_1-\delta_2)/(1+2\delta_2).\end{aligned} \qquad (11)$$

the first two rows of matrix $\mathbf{G}$ become zero. This is the elliptic anisotropy condition for orthorhombic media. The conditional damping is an alternative approach to remove the S-wave noise without altering the anisotropy model. The attenuation is time dependent and is effective for later times. To remove early time S-wave noise, the elliptic anisotropy method should also be implemented.

EXAMPLES

Figure 1 shows wavefield snapshots using four different finite-difference implementations. The model is a 6 km x 6 km x 6 km cube of constant velocity 2 km/s. The anisotropy parameters are $\varepsilon_1 = 0.2$, $\varepsilon_2 = 0.12$, $\delta_1 = \delta_2 = 0.06$, and $\delta_3 = 0$. The tilt angles are $\theta = 45°$, $\phi = \beta = 0$. The source is a Ricker wavelet of 15 Hz peak frequency. The grid spacing is 20 m.

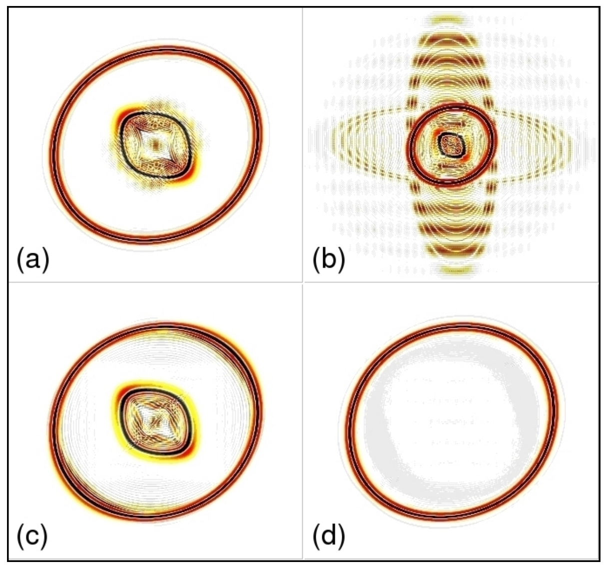

Figure 1: Wavefield snapshot of a homogeneous orthorhombic model using (a) direct finite-difference implementation of equation (1), (b) self-adjoint first-derivative implementation by centered finite-difference, (c) self-adjoint first-derivative implementation by staggered finite-difference without wavefield interpolation, (d) selective damping with equation (7).

Figure 1a shows a wavefield snapshot at time 1.0 s at a vertical plane crossing through the model center. It was computed using direct implementation of equations (1) to (6). The finite-difference method uses optimized 16th order coefficients. Note the large amplitude source-generated S-wave noise at the center. The noise grows as propagation time increases and destroys the solution.

As mentioned previously, Zhang and Zhang (2011) implemented it using the self-adjoint operator in equation (3). They evaluated the first derivatives using centered finite-difference method. Figure 1b shows the wavefield snapshot at 0.4 s using this method. The first derivatives are computed using 8th order optimized centered finite-difference scheme. Note the high velocity, high frequency elliptic artifacts due to an inaccurate

DOI http://dx.doi.org/10.1190/segam2014-1290.1

derivative to the difference approximation. To reduce the artifacts, Zhang et al. (2011) proposed to use a pseudospectral method or an *extremely high order* finite-difference method.

The high-frequency artifacts can be avoided by using a staggered finite-difference expansion of the first derivatives. However, the wavefield as well as the physical properties must be interpolated at the center of the staggered location. Without these interpolations, the solution is dispersive, especially at high frequency. Figure 1c shows the wavefield snapshot at 1.0 s using the staggered finite-difference implementation of the self-adjoint operator of equation (3). In this method, the wavefield is not interpolated. Instead, the wavefield at the nearest point is borrowed. This method gives a stable solution. However it is inaccurate. The P-wave wavefront at the high velocity direction is dispersive. The dispersion can be noticed by comparing with Figure 1a.

Figure 1d shows a wavefield snapshot using selective damping given in equation (7). It gives stable solution. Also the S-wave noise is removed. Note that early time S-wave noise is not removed effectively.

Figure 2 shows impulse response of an orthorhombic model. The model is a homogeneous 10 km x 10 km x 5 km cube with grid spacing of 20 m. The anisotropic parameters and tilt angles are same as the model given in Zhang and Zhang (2011), i.e., $V_p = 2000$ m/s, $\varepsilon_1 = 0.2$, $\varepsilon_2 = 0.12$, $\delta_1 = \delta_2 = 0.06$, $\delta_3 = 0$. The tilt angles are $\theta = 40°$, $\phi = 35°$, $\beta = 25°$. The input is a trace of three impulses at $t = 2, 3, 4$ s. The source wavelet has a bandwidth of 1-2-15-20 Hz. The source and impulse trace are located at the surface of the model center. I modified the anisotropy parameter so that the orthorhombic elliptic anisotropy condition, given in equation (11), is satisfied up to 0.5 times the peak wavelength from the source point, and gradually tapered out up to another such distance. This combined with the selective S-wave damping method effectively removes source generated S-wave noise. I applied very mild 3D low-wavenumber filter to remove residual RTM noise.

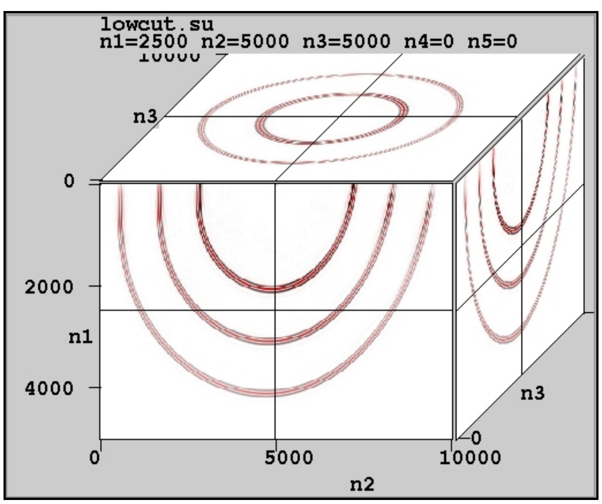

Figure 2: RTM impulse response of a tilted-orthorhombic homogeneous model.

There is a notable difference between this and the impulse response presented by Zhang and Zhang (2011), especially in the shallow section. Figure 2 shows a nice migration smile with correct tilt behavior from bottom to top with almost uniform amplitude. However, the published impulse response decayed rapidly in the shallow section. I believe the current improvement is primarily due to removing the source-generated S-wave noise successfully.

Figure 3 (next page) shows a Gulf of Mexico field data example. The data is a composite of two orthogonal wide-azimuth surveys as described in Baldock et al. (2011). The velocity and anisotropy parameters are determined by a multi-azimuth TTI tomography analysis as described in He et al. (2013). Figure 3a is a section of TTI RTM image. Figure 3b is an orthorhombic RTM image of the same area. The highlighted area shows improved reflection in the orthorhombic image.

Figure 4 shows the RTM azimuth angle gather at the highlighted area. The left panel is the TTI RTM gather, and the right panel is the orthorhombic RTM gather. Each panel has six azimuth angle gathers from 0 to 150 degrees with a 30 degree increment. The left (TTI) panel shows orthorhombic anisotropy by the different residual moveout between the gathers. The residual moveout has been successfully flattened on the right (orthorhombic) panel.

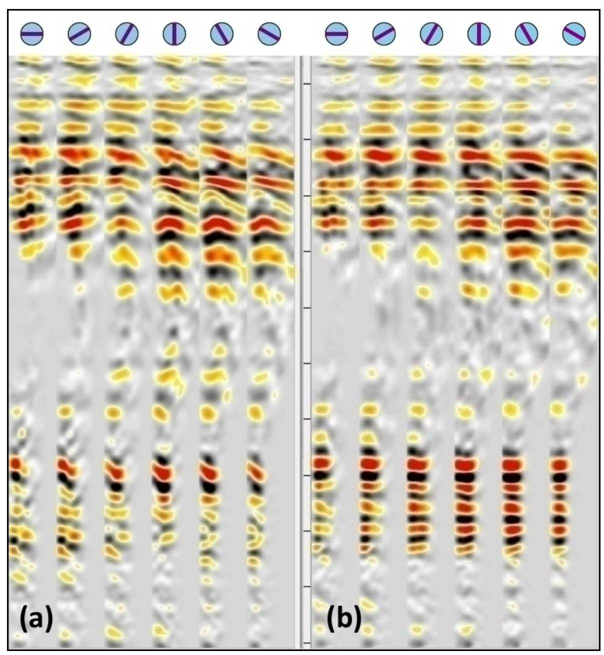

Figure 4: Azimuth-angle gather comparison between (a) TTI and (b) orthorhombic RTM.

CONCLUSIONS

A new finite-difference implementation method for orthorhombic RTM is proposed. The method is based on locally constant tilt angles. By ignoring the spatial derivative of angles the wave equation is greatly simplified. However, the simple finite-difference implementation is unstable.

DOI http://dx.doi.org/10.1190/segam2014-1290.1

I have introduced a conditional damping term to the simplified wave equation which gives a stable solution and reduced S-wave noise at later times. An orthorhombic elliptic anisotropy condition is derived and implemented around the source point to reduce the source generated S-wave noise in the shallow section. Numerical tests show that the proposed method is effective. The method is applied on an orthorhombic RTM of a sample Gulf of Mexico data. The result is a better image than previous TTI RTM image.

ACKNOWLEGEMENTS

I thank Jean Ji for preprocessing field seismic data, Yang He for providing the orthorhombic anisotropy model. I thank James Sheng, Bin Wang, Zhiming Li and Connie VanSchuyver for reviewing the paper. I thank TGS management for permission to publish this paper.

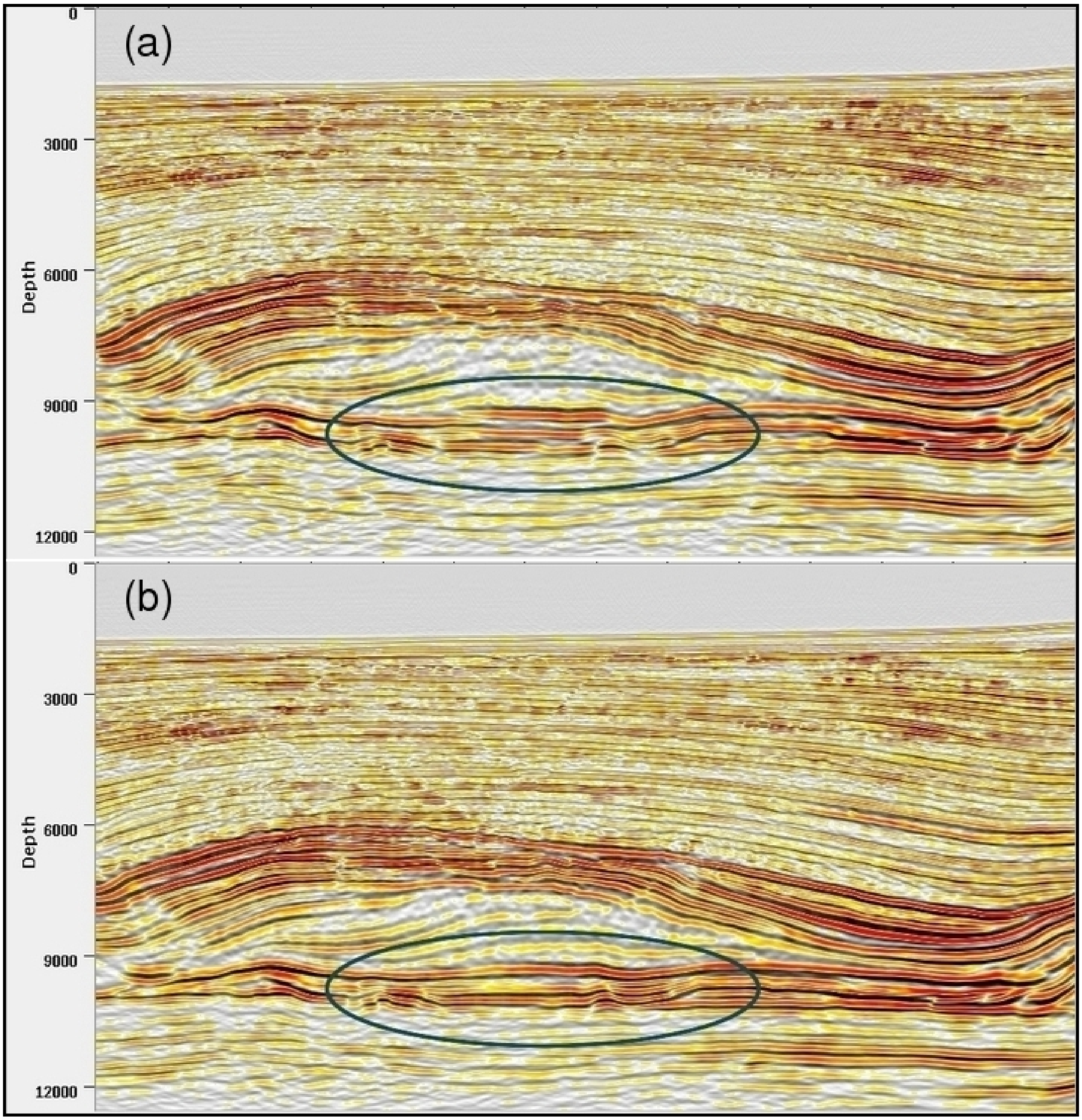

Figure 3: A comparison of (a) TTI RTM and (b) orthorhombic RTM images.

DOI http://dx.doi.org/10.1190/segam2014-1290.1

http://dx.doi.org/10.1190/segam2014-1290.1

EDITED REFERENCES

Note: This reference list is a copy-edited version of the reference list submitted by the author. Reference lists for the 2014 SEG Technical Program Expanded Abstracts have been copy edited so that references provided with the online metadata for each paper will achieve a high degree of linking to cited sources that appear on the Web.

REFERENCES

Baldock, S., C. Reta-Tang, B. Beck, W. Gao, E. Doue, and S. Hightower, 2011, Orthorgonal wide azimuth surveys: Acquisition and imaging: 81st Annual International Meeting, SEG, Expanded Abstracts, 147–151.

Duveneck, E., and P. M. Bakker, 2011, Stable P-wave modeling for reverse-time migration in tilted TI media: Geophysics, **76**, no. 2, S65–S75, http://dx.doi.org/10.1190/1.3533964.

He, Y., A. Gersztenkorn, G. Hilburn, S. Yang, and B. Wang, 2013, Orthorhombic PSDM processing, a case history in Mississippi Canyon, Gulf of Mexico: 83rd Annual International Meeting, SEG Expanded Abstracts, 3799–3803.

Holberg, O., 1987, Computational aspects of the choice of operator and sampling interval for numerical differentiation in large-scale simulation of wave phenomena: Geophysical Prospecting, **35**, no. 6, 629–655, http://dx.doi.org/10.1111/j.1365-2478.1987.tb00841.x.

Kindelan, M., A. Kamel, and P. Sguazzero, 1990, On the construction and efficiency of staggered numerical differentiators for the wave equation: Geophysics, **55**, 107–110, http://dx.doi.org/10.1190/1.1442763.

Thomsen, L., 1986, Weak elastic anisotropy: Geophysics, **51**, 1954–1966, http://dx.doi.org/10.1190/1.1442051.

Tsvankin, I., 1997, Anisotropic parameters and P-wave velocity for orthorhombic media: Geophysics, **62**, 1292–1309, http://dx.doi.org/10.1190/1.1444231.

Zhang, H., and Y. Zhang, 2011, Reverse-time migration in vertical and tilted orthorhombic media: 81st Annual International Meeting, SEG Expanded Abstracts, 185–189.

Zhang, Y., H. Zhang, and G. Zhang, 2011, A stable TTI reverse time migration and its implementation: Geophysics, **76**, no. 3, WA3–WA11, http://dx.doi.org/10.1190/1.3554411.